

Supporting Information

Localized Gelation Cellulose Separators Enables Dendrite-free Anodes for the Future-Oriented Zinc Ion Battery

Chenpeng Xi^a, Yuanbin Xiao^a, Chengkai Yang^{a,*}, Mengchao Li^a, Long Li^a, Yu Chao^a, Lingyun Li^{a,*}, Chunnian He^b, Yan Yu^{a,*}

^a Key Laboratory of Advanced Materials Technologies, International (HongKong Macao and Taiwan) Joint Laboratory on Advanced Materials Technologies, College of Materials Science and Engineering, Fuzhou University, Fuzhou, Fujian, 350108, China

^b School of Materials Science and Engineering, Tianjin University, Tianjin, 300072, China

*Corresponding mails: chengkai_yang@fzu.edu.cn (C.K. Yang), lilingyun@fzu.edu.cn (L.L. Li), yuyan@fzu.edu.cn (Y. Yu).

Experimental section

1. Preparation process of Cellulose solution

All materials were used according to the specifications at the time of purchase, and no additional processes were performed. Take 200 ml of pure water and cool it to 0°C and divide it into two parts A and B. Add 8g of urea to A, stir until completely dissolved and reserve for later. Place B in an ice water bath, slowly add 5 g of NaOH and stir continuously until the solid is completely dissolved and wait until the solution is cooled to room temperature. Add 4 g of cotton to B and stir vigorously for five minutes until the liquid has good flow. Add solution A to B and continue stirring for 5 min. The resulting solution was sealed and left to stand for 30 min. Add 100 ml of pure water to the rested mixed solution and mix thoroughly until homogeneous.

2. Preparation process of LGS

Take a square Teflon tank with the size of 150mm*200mm*50mm. After pouring the cellulose solution into the Teflon tank, the Teflon tank was placed in suspension over water and ultrasonic for 10 minutes. Keeping the ultrasonic on, use a spray bottle to spray 1M H₂SO₄ into the Teflon tank until no more bubbles are produced after the new sulfuric acid is sprayed. The Teflon tank was removed and the contents were washed with an excess of pure water. Measured using pH paper, the contents should be neutral. After pressing out the excess water, the resulting film is folded in half twice and pressed firmly. The pressed film is placed in a blast oven at 80°C and dried for 12 hours. The dried membranes are cut into 16 mm diameter discs using a hole punch. Each time the process is performed, 150-200 sheets of film can be obtained. Add 25 µl of 1 M ZnSO₄ solution to each disc at the time of use. After adding electrolyte, the membrane becomes LGS. After assembling the battery with LGS, it needs to be left for more than 2 hours to ensure that the system achieves uniformity and stability.

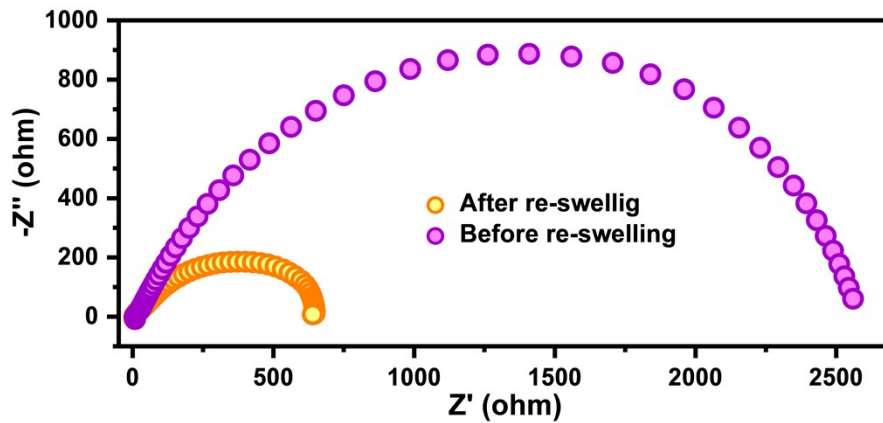


Figure S1 Impedance spectrum of a zinc symmetric cell using LGS, before and after refilling electrolyte.

The gradual increase of R_{ct} is mainly used to illustrate the gelation process of cellulose. We added far less electrolyte to the cellulose than was needed for adequate swelling. Cellulose continuously absorbs electrolyte during the dissolution process, resulting in electrolyte deficiency at the interface. The absence of electrolyte leads to an increase in interfacial impedance, demonstrating the presence of gelation. It is generally believed that an increase in R_{ct} reduces the performance of the battery, but our study found that this is not absolute. The value of R_{ct} in Figure 2a is large, but this is only the data measured without polarization voltage. When the battery is operating, there is a polarization voltage at both ends of the battery, which can lower the R_{ct} . If the value of R_{ct} after applying polarization is not high, it will not affect the working condition of the battery. In addition, a certain inhibitory effect can avoid excessive growth of dendrites. So all in all we think this effect is beneficial.

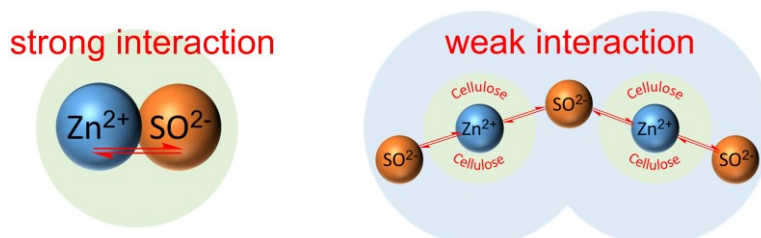


Figure S2 Schematic diagram of the principle of displacement of XPS peak to low binding energy.

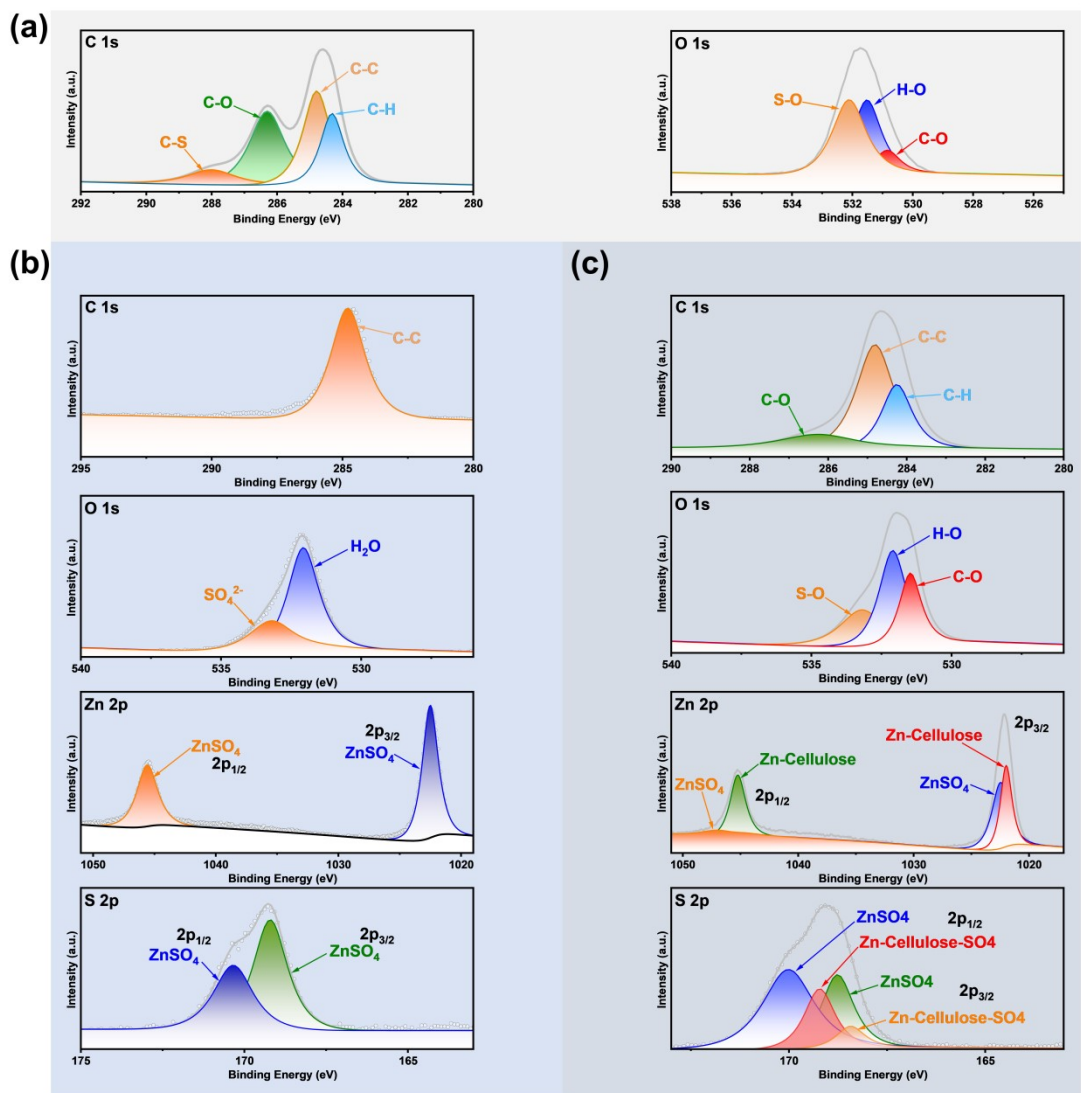


Figure S3 (a) XPS pattern of dried cellulose septum. (b) XPS pattern of zinc sulfate. (c) XPS pattern of LGS

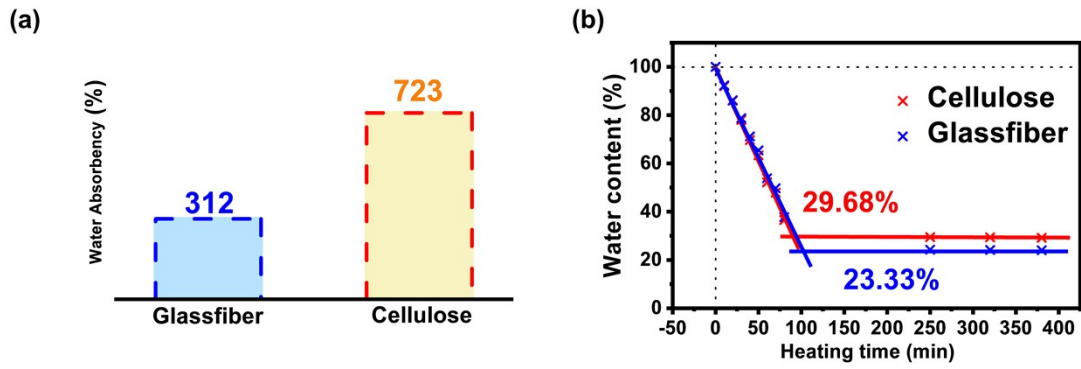


Figure S4 (a) Water absorption of the two separators. (b) The percentage of combined water for the two separators.

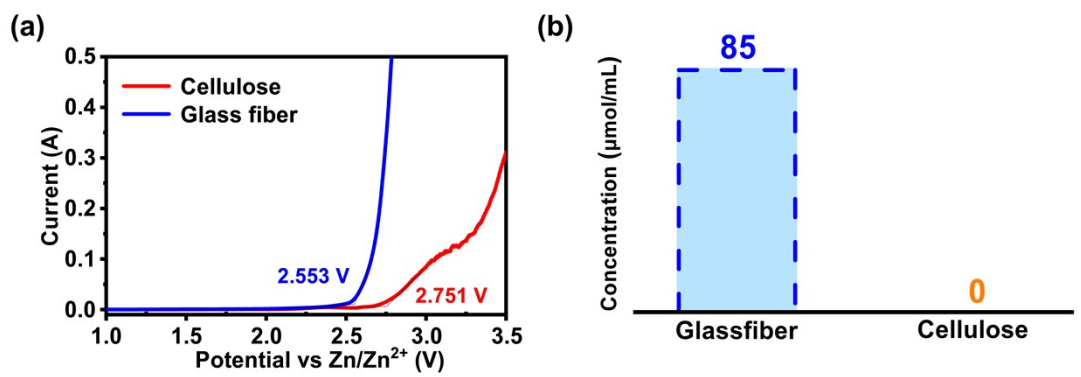


Figure S5 (a) Electrochemical stabilization windows for two separators. (b) Hydrogen production for different electrolytes.

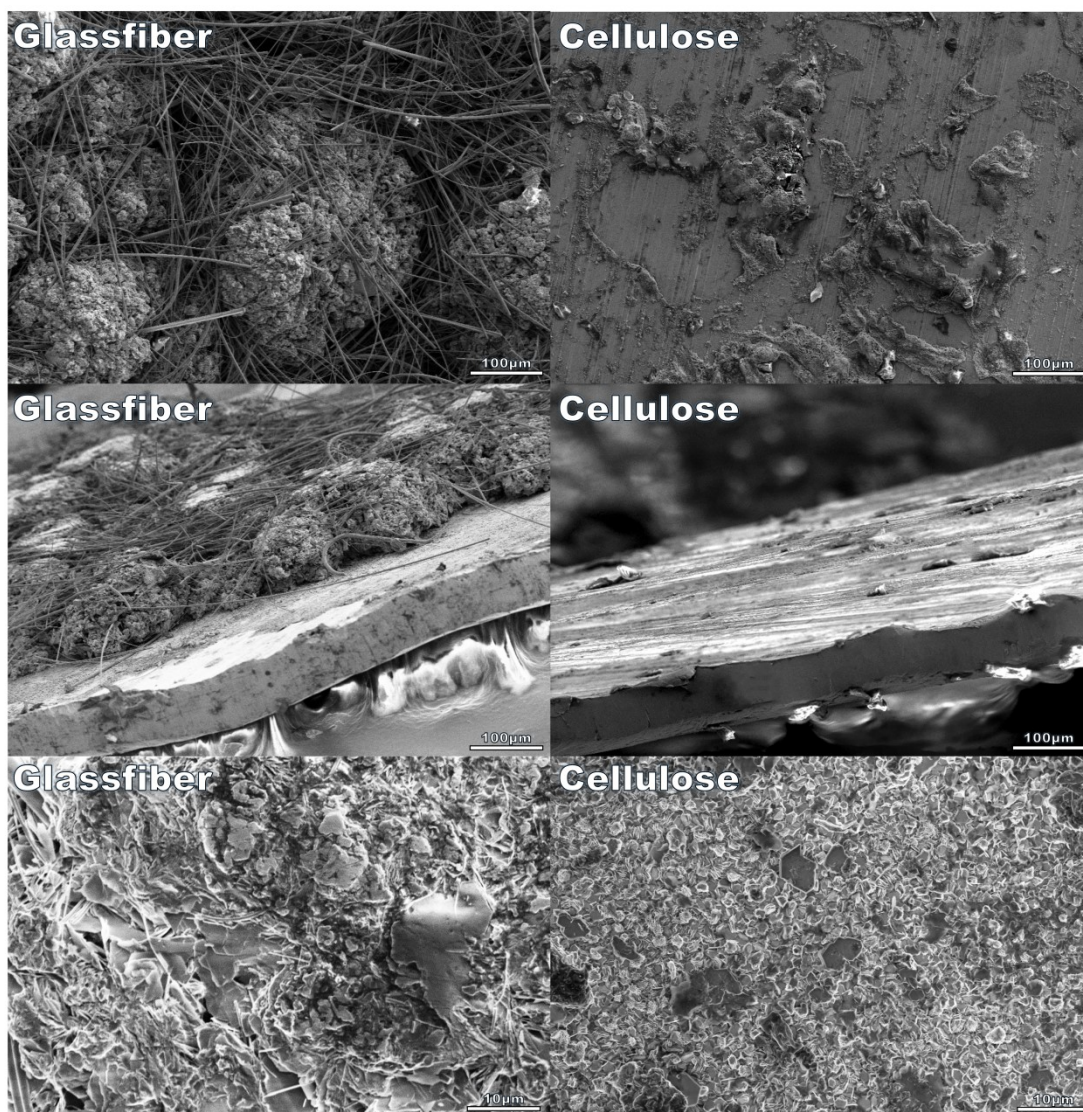


Figure S6 SEM images of dendrite morphology after deposition using glass fiber separators and LGS assembly for zinc symmetric cells, respectively

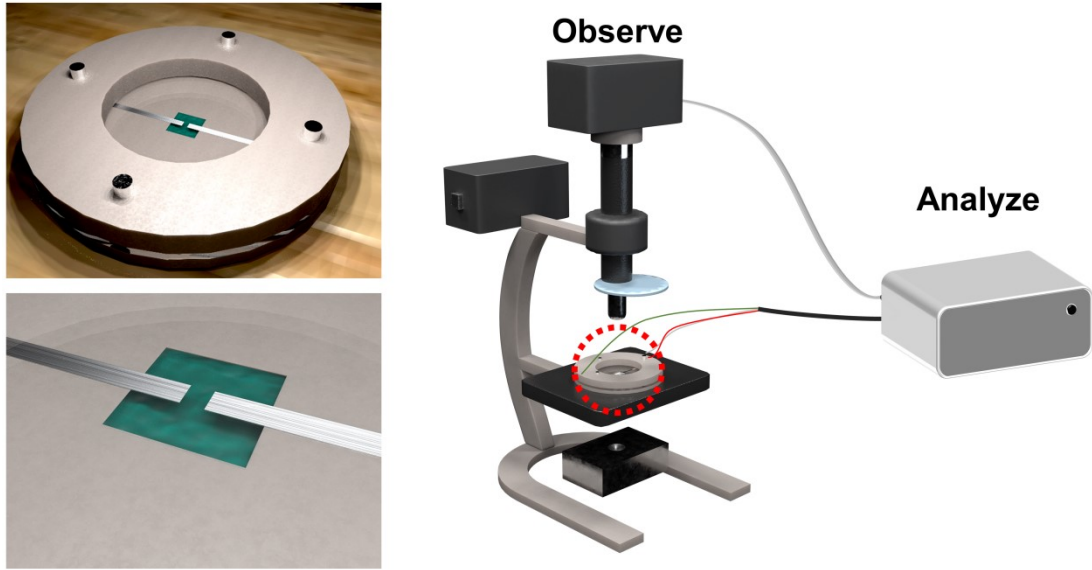


Figure S7 Schematic diagram of in situ dendrite observation device

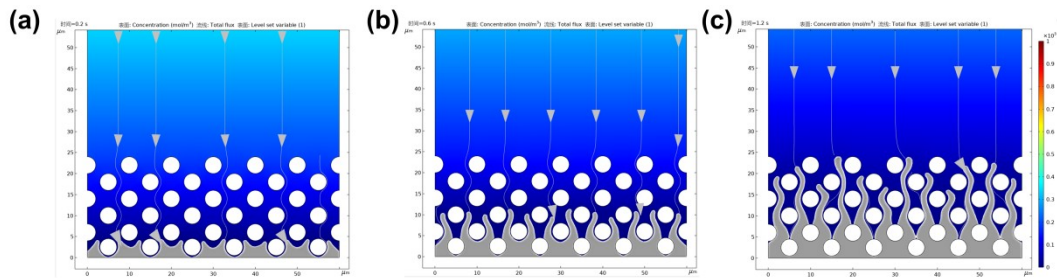


Figure S8 (a-c) Simulation of dendrite growth in a Zn-symmetric cell using glass fibers as a diaphragm, using COMSOL multiphysics 5.6 as the platform.

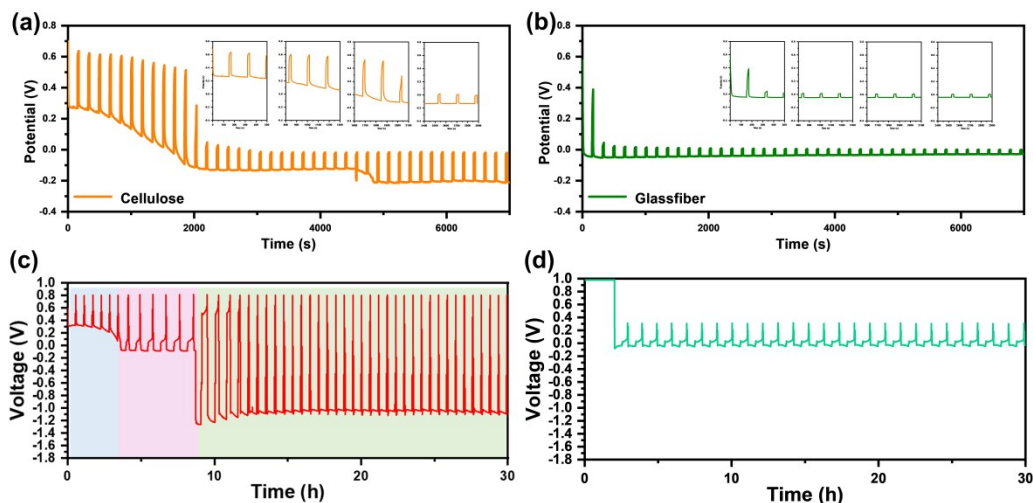


Figure S9 (a-b) Galvanostatic Intermittent Titration Technique (GITT) test of Zn-Cu cells with glass fiber separators and LGS. (c-d) Cullen Efficiency test data of Zn-Cu cell with glass fiber separators and LGS.

Zn-Cu cells will get a different result if the dendrite growth pattern in LGS is different from that in LE. We speculate that the LGS regulates the dendrites by controlling the motion of the fibers. **Figure S9a, S9b** is the test data of Zn-Cu cells with glass fiber separators and LGS using Galvanostatic Intermittent Titration Technique (GITT). It can be clearly seen in **Figure S9a** that several distinct stages have been experienced from the initial state to the final steady state. The relaxation voltage in **Figure S9b** drops rapidly to zero volts, which indicates that the available copper working surface is consumed in a very short time, corresponding to the immutable interface between the electrode and the separator brought by the glass fiber. When the copper working surface is completely depleted, the relaxation voltage goes to zero since the poles are the same metal. In LGS, not all electrode surfaces are working surfaces at the beginning since the ion transport part exists only in the part where the fibers are in contact with the electrodes. When the dendrites grow, the existing working surfaces disappear, the fibers are topped off and new working surfaces are created. This leads to the fact that the relaxation voltage will not be able to drop to the zero level until the copper electrode is completely covered with zinc, which is shown in **Figure S9a**.

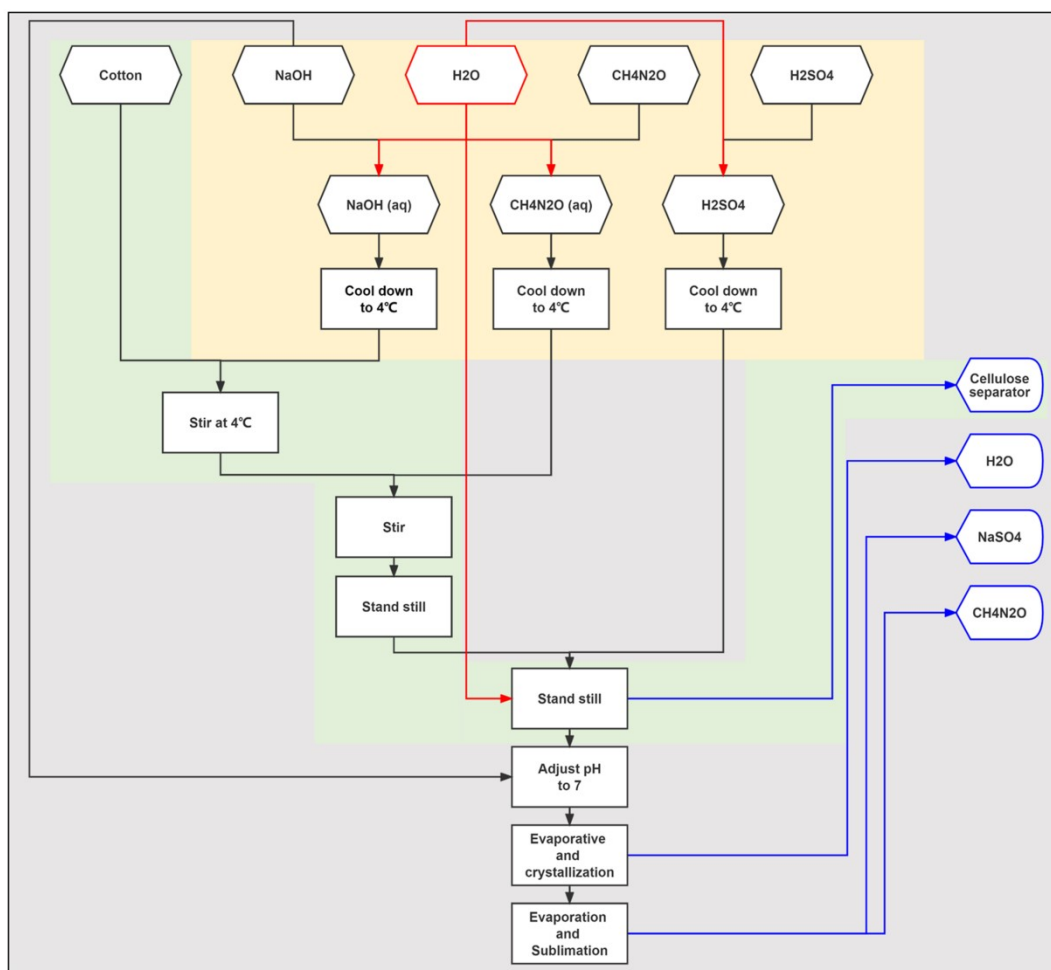


Figure S10 Material-process flow block diagram for the harmless preparation of LGS

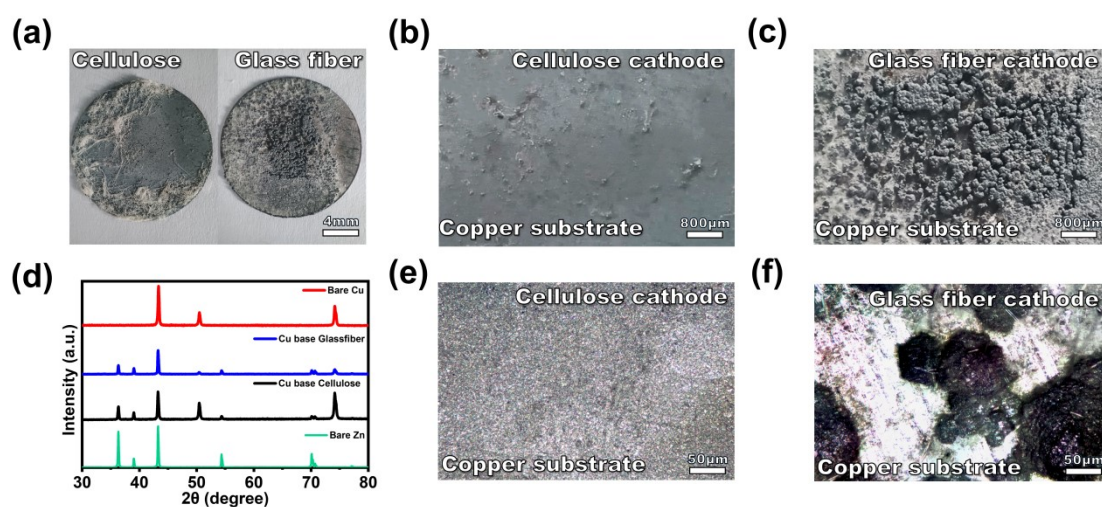


Figure S11 (a) Using different separators for zinc-copper cells, the deposited copper sheets are stripped out and photographed (b-c) Using different separators for

zinc-copper cells, the deposited copper sheets are stripped out and photographed (d) Using different separators for zinc-copper cells, the deposited copper flakes are stripped out and analyzed by XRD (e-f) Using different separators for zinc-copper cells, the deposited copper sheets are stripped out and photographed.

Some studies have suggested that the effect on dendrite growth may originate at the microscopic level, and that dendrites are milder when certain crystalline surfaces with a more horizontal growth direction are increased. After analysis, it was found that zinc dendrites in cells using LGS and glass fiber diaphragms did not reflect such a difference (**Figure S11**). So the variation in dendrite growth should be mainly influenced by more macroscopic effects. This further validates the effectiveness of the local gelation strategy.

The intent of this test is to verify the effect of LGS on the crystal orientation of dendrite growth. If a zinc sheet is used as the substrate, it will be difficult to distinguish the substrate signal from the dendrite signal. The high hardness of the zinc sheet makes it difficult to peel off the dendrites. Therefore, we chose copper substrates so that the obtained zinc crystal signals all originate from the newly grown dendrites. This allows us to precisely analyze the changes in crystal orientation by XRD.

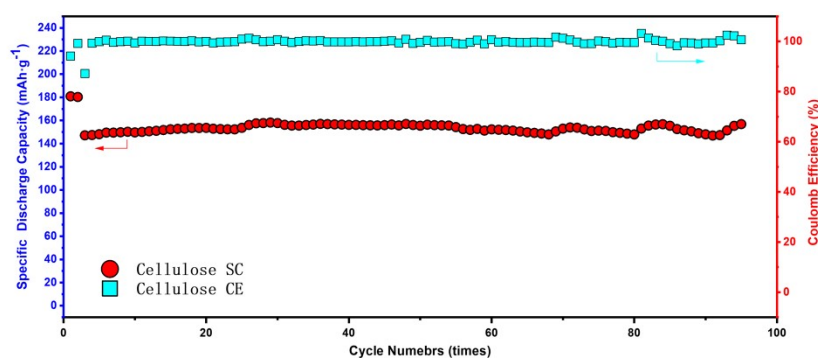


Figure S12 Cycle performance of Li/LGS/LFP cells at 1C rate